Electronic Supplementary Material (ESI) for Materials Horizons.

Supporting Information

Are the Rates of Dexter Transfer in TADF Hyperfluorescence Systems Optically Accessible?

*Nils Haase** [a,b]*, Andrew Danos** [c]*, Christof Pflumm*[b] *, Patrycja Stachelek*[c]*, Wolfgang Brütting*[a]*, and Andrew P. Monkman*[c]

[a] Institute of Physics, Experimental Physics IV, University of Augsburg, Universitätsstr. 1, 86135 Augsburg, Germany

[b] Merck KGaA, Display Solutions, Frankfurter Straße 250, 64293 Darmstadt, Germany

[c] Department of Physics, Durham University, South Road, DH1 3LE, UK

*Email: nils.haase@merckgroup.com
*Email: andrew.danos@durham.ac.uk

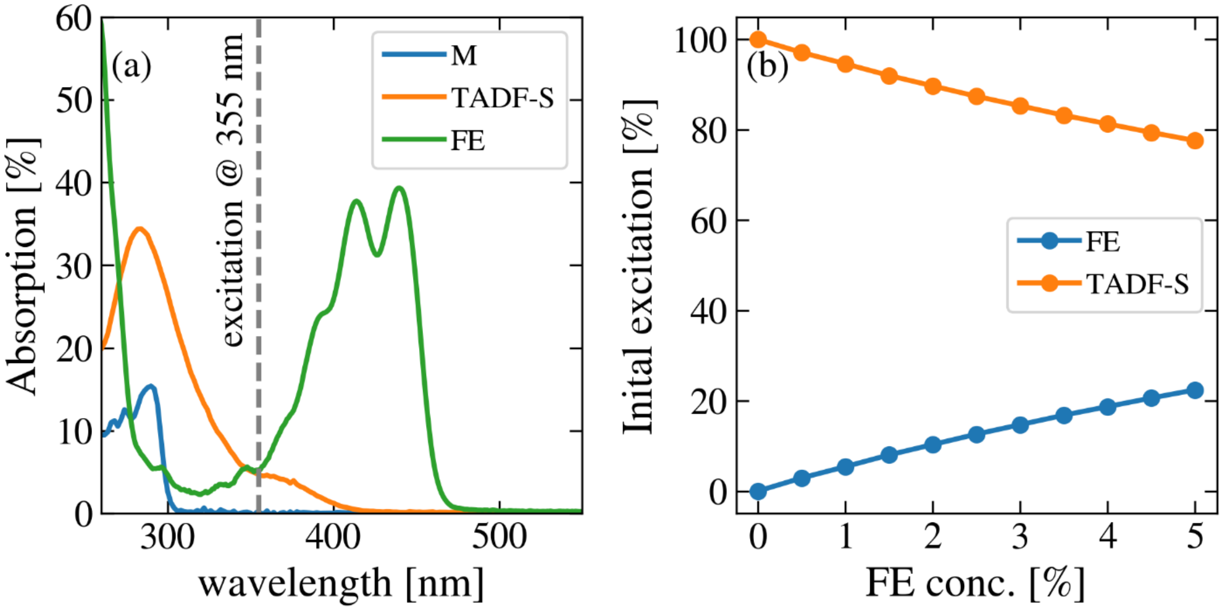

Figure S1: (a) Absorption of 50nm neat films of DPEPO (M), DDMA-TXO2 (TADF-S) and TBPE (FE). The grey dotted line represents the excitation wavelength of the TRPL and PLQE experiments. (b) Calculated concentration dependent initial excitation of both the TADF-S as well as the FE in mixed films of M:TADF-S(20%):FE(x%).

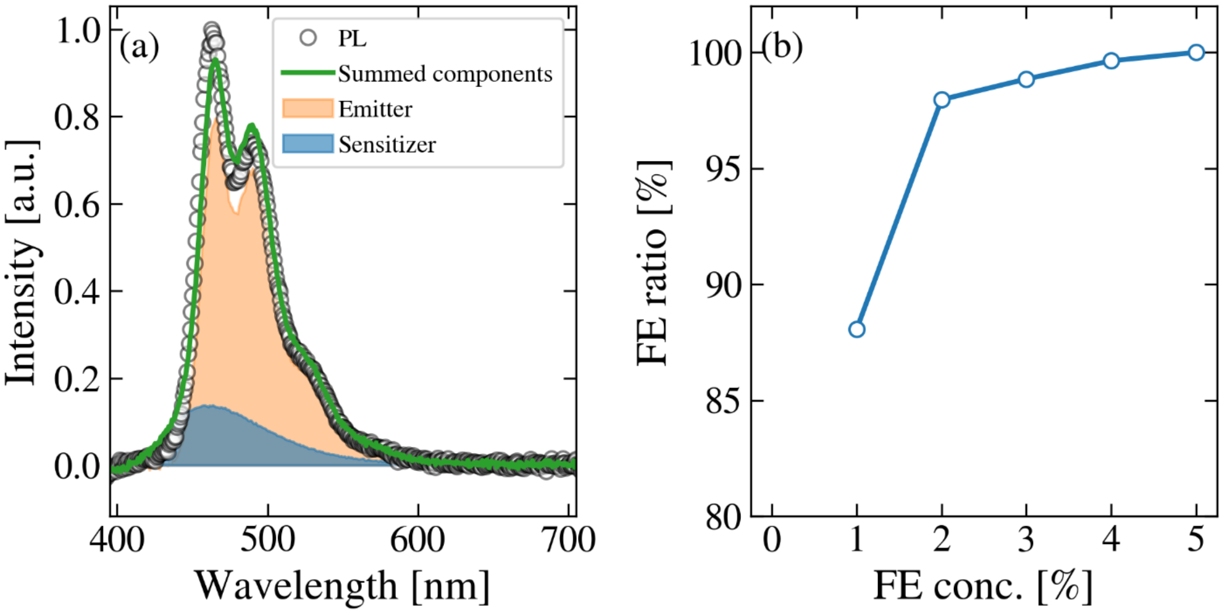

Figure S2: (a) Normalized PL spectrum of M:TADF-S(20%):FE(1%) resolved into its TADF-S and FE components. (b) Contribution of the FE emission to the PL spectrum depending on the FE concentration. Even at low doping level of 2% nearly 98% of the total emission originates from the FE, although it absorbs less than 20% of the excitation (Figure S1b).

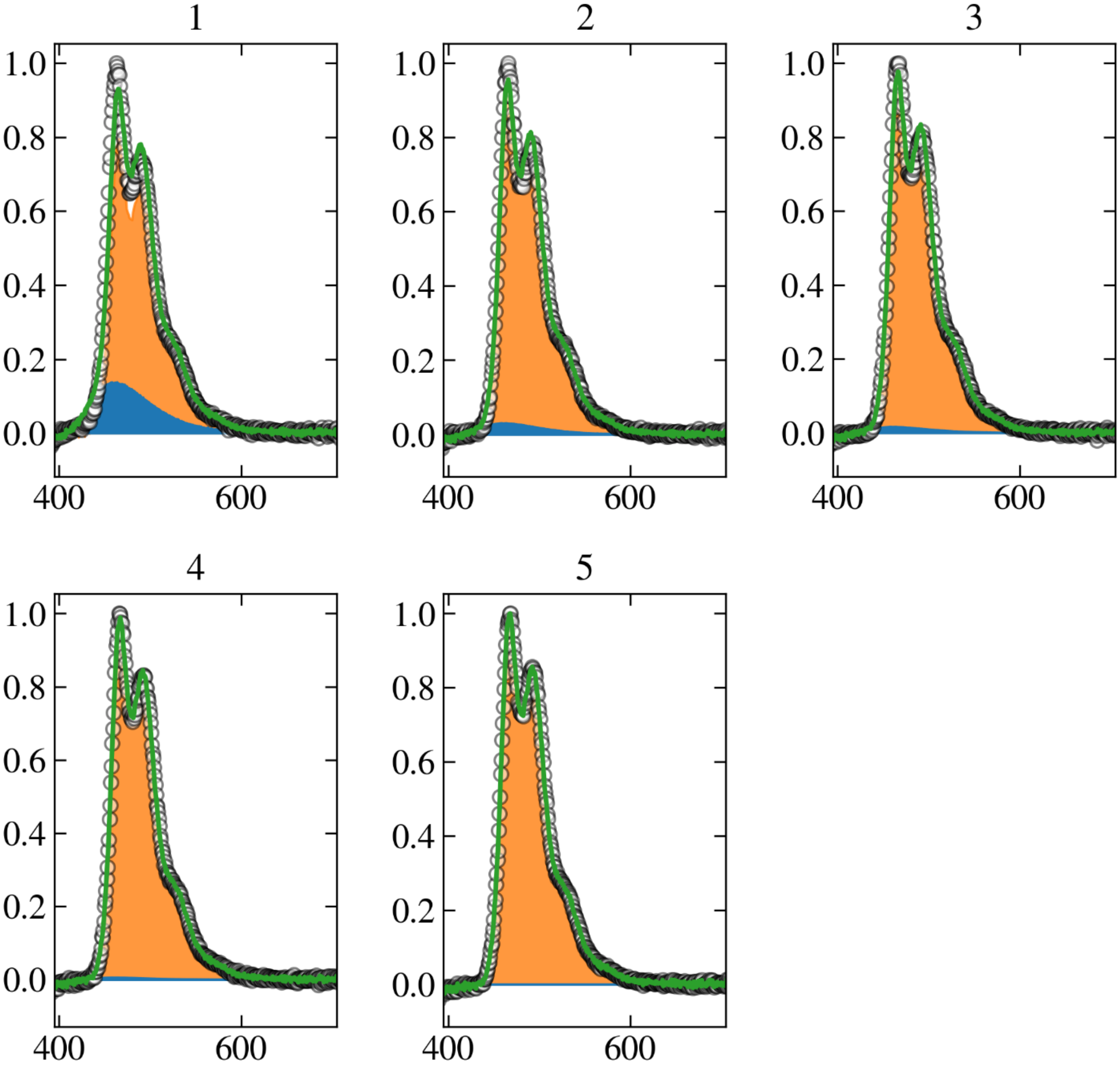

Figure S3: Steady-state PL spectra (355 nm excitation) of hyperfluorescent films with different FE loadings (above each panel). The contributions to total emission from the TADF-S (blue) and FE (orange) are displayed flowing deconvolution using known spectra of the individual components.

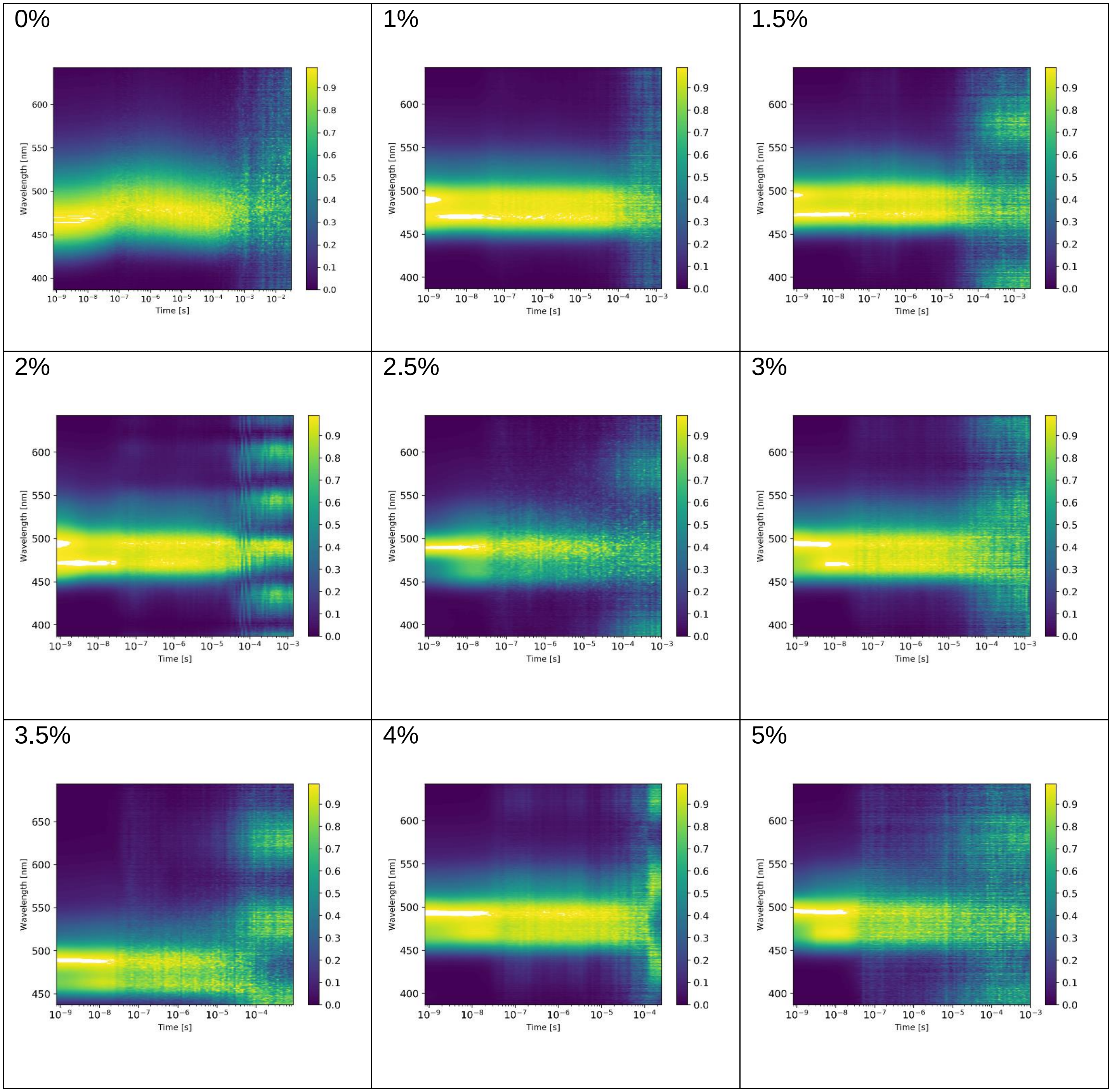

Figure S4: Peak normalised time-resolved emission spectra of M:TADF-S(20%):FE(x%) films. The vibronic features of the FE emission band dominate at all times and at all concentrations. Significant changes in the spectral shape (eg, 2% sample at >100 µs, 3.5% sample at >50 µs) occur when the emission signal strength falls below the noise floor of the instrument, resulting instead in normalization of the baseline.

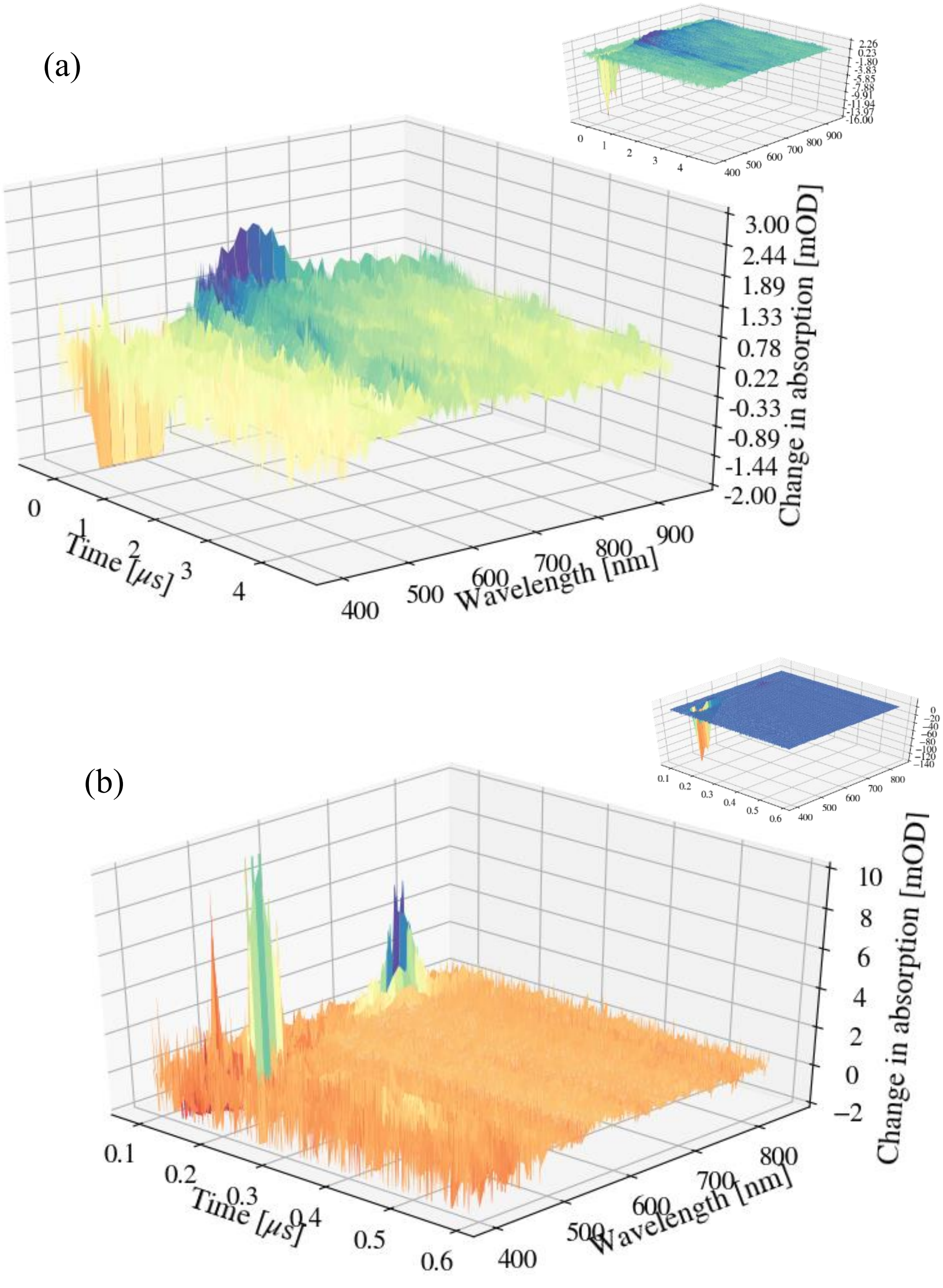

Figure S5: Transient absorption maps of (a) M:TADF-S(20%) and (b) M:TADF-S(20%):FE(2%). While a long lived excited state absorption is observed at around 600 nm for M:TADF-S(20%) it vanishes upon adding 2% FE (note the difference in time axis scales). Full-scale insets reveal large amplitude short-lived negative features in each TA map, attributed to pump-induced emission of the TADF-S (a) or FE (b). The additional short-lived positive feature at 530nm in (b) is an artefact also associated with pump-induced emission (see Figure S7, TA map).

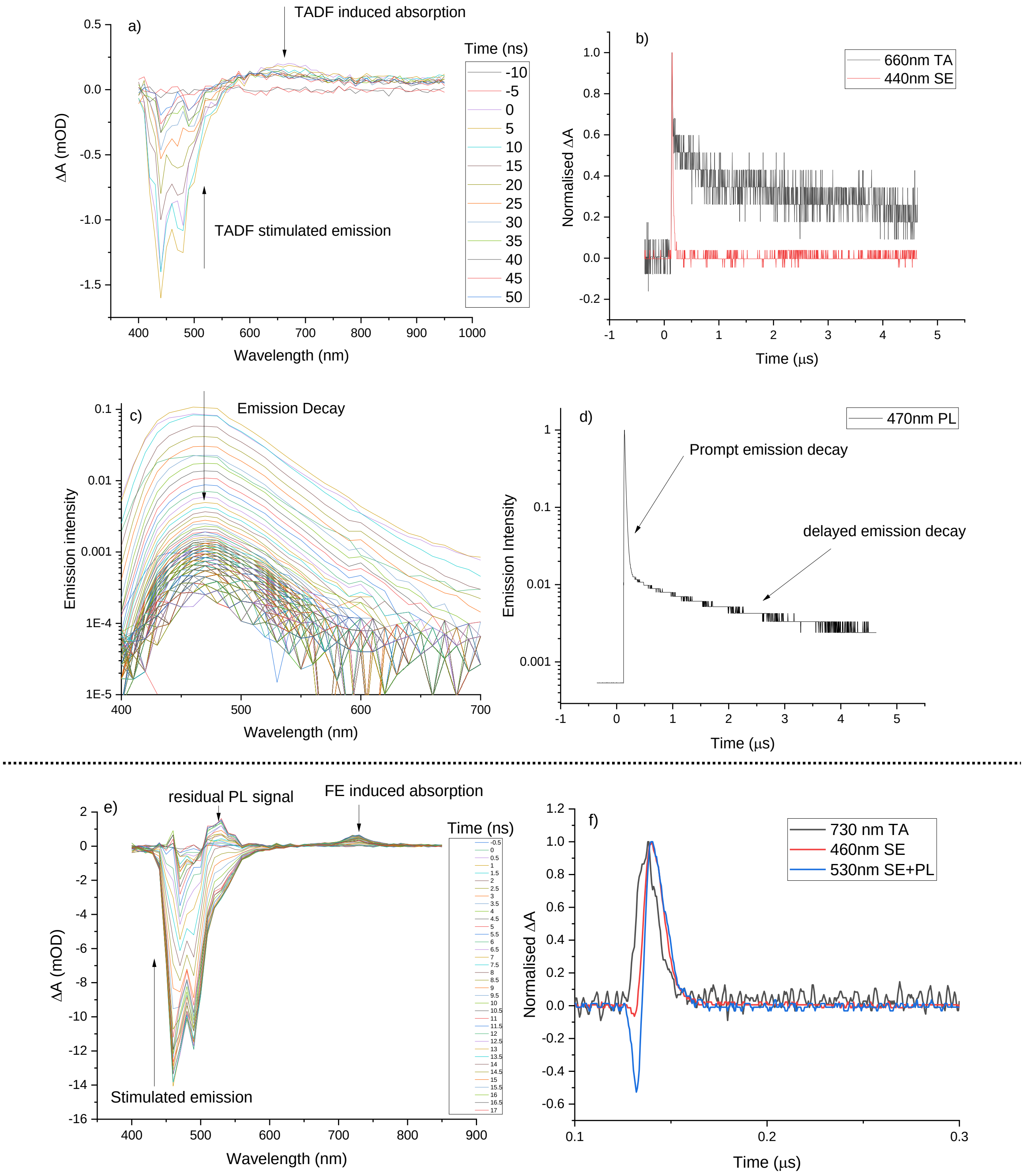
a)
TADF induced absorption
TADF stimulated emission
ΔA (mOD)
0.5
0.0
-0.5
-1.0
-1.5
Wavelength (nm)
400
500
600
700
800
900
1000
Time (ns)
-10
-5
0
5
10
15
20
25
30
35
40
45
50
b)
660nm TA
440nm SE
Normalised ΔA
1.0
0.8
0.6
0.4
0.2
0.0
-0.2
Time (μs)
-1
0
1
2
3
4
5
c)
Emission Decay
Emission intensity
0.1
0.01
0.001
1E-4
1E-5
Wavelength (nm)
400
500
600
700
d)
470nm PL
Prompt emission decay
delayed emission decay
Emission Intensity
1
0.1
0.01
0.001
Time (μs)
-1
0
1
2
3
4
5
e)
residual PL signal
FE induced absorption
Stimulated emission
ΔA (mOD)
2
0
-2
-4
-6
-8
-10
-12
-14
-16
Wavelength (nm)
400
500
600
700
800
900
Time (ns)
-0.5
0
0.5
1
1.5
2
2.5
3
3.5
4
4.5
5
5.5
6
6.5
7
7.5
8
8.5
9
9.5
10
10.5
11
11.5
12
12.5
13
13.5
14
14.5
15
15.5
16
16.5
17
f)
730 nm TA
460nm SE
530nm SE+PL
Normalised ΔA
1.2
1.0
0.8
0.6
0.4
0.2
0.0
-0.2
-0.4
-0.6
Time (μs)
0.1
0.2
0.3

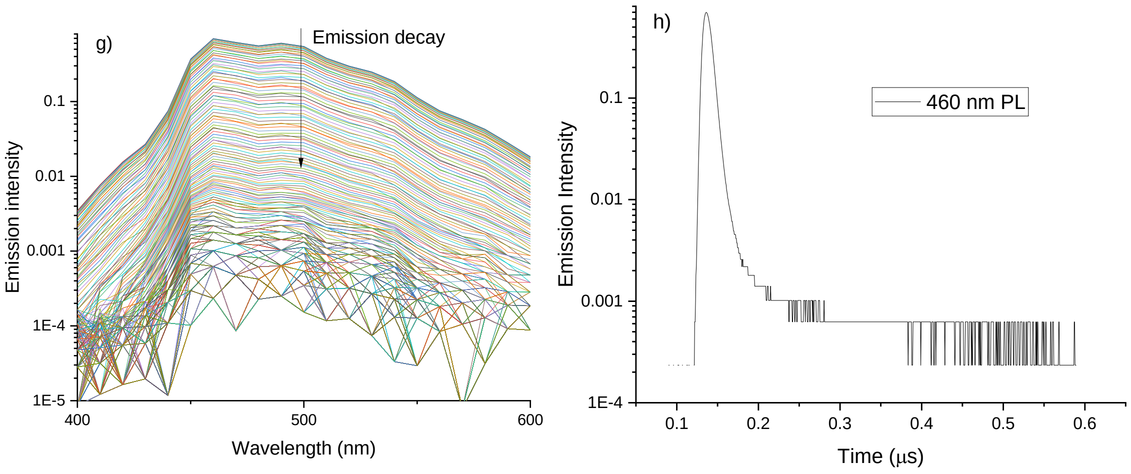

Figure S6: Additional decays and spectra of transient absorption and time-resolved PL (collected on same instrument) in TADF-only (a-d) and hyperfluorescent films (e-h). Spectra in c) and g) correspond to those in Figure S4 (0% and 2% FE).

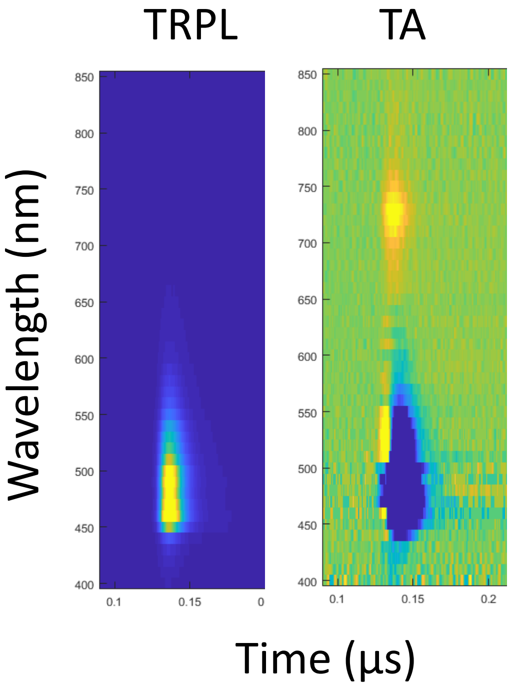

Figure S7: Comparison of photoluminescence signal (pump only) with transient absorption signal (pump and probe) for M:TADF-S(20%):FE(2%), both recorded simultaneously on same sample and instrument. The positive prompt emission feature in the TRPL (yellow band, 450-550nm) is matched by strong a negative feature in the TA spectrum (blue band, saturated on colour scale to allow observation of significantly smaller TA band at longer wavelengths). The short lived positive (yellow) feature at ~530nm in the TA map is due to timing jitter in the subtraction of the pump-induced PL signal. The additional induced absorption feature in the TA data (650-800nm) decays on the same timescale as the TRPL, and is attributed to S_1 to S_2 absorption of the TBPe.

FRET RATE CALCULATION

$$k_{FRET} = \frac{1}{\tau_D}\left(\frac{R_{FRET}}{r}\right)^6 = \frac{1}{\tau_D r^6}\frac{9000\ln(10)\,\kappa^2\,\Phi_D}{128\,\pi^5 N_A n^4}J(\lambda) \qquad (1)$$

$$J(\lambda) = \int_0^\infty \epsilon_A(\lambda)\;\cdot\lambda^4\cdot Em_D(\lambda)\cdot d\lambda \qquad (2)$$

Both the expected rate of FRET (k_{FRET}) and the FRET radius (R_{FRET}) can be calculated with equations (1) and (2); from direct measurements of the energy donor emission lifetime ($\tau_D = 25$ ns, see main text), and using κ = 2/3 for a random ensemble of orientations, $\Phi_D = 0.85$[40], and n = 1.7 for the refractive index of the DPEPO host.

The molar extinction coefficient of the energy acceptor ($\epsilon_A(\lambda)$) can be estimated from the absorption spectrum of FE dissolved in toluene at low concentration using $\epsilon = \frac{E}{cd}$, where ϵ is the molar extinction coefficient, E the dimensionless extinction, c the substance concentration and d the thickness of the cuvette. In principle it is also possible to use film absorption measurements however it is not straightforward to determine the molar concentration of the material in thin films. No spectral shift in the absorption could be found between solution and film measurements with low FE concentrations in an inert matrix.

J(λ) in equation (2) is the spectral overlap integral (green shaded area, Figure 2b), calculated from the of the area-normalised donor emission spectrum ($Em_D(\lambda)$) and the molar extinction spectrum of the acceptor.

NUMERICAL MODELLING OF PLQE RESULTS

Model Equation - Adopting the analysis methods of Dias et al (Dias *et al* 2017 *Methods Appl. Fluoresc.* **5** 012001), we first express the total PLQE from the TADF material (Φ_{TADF}) in terms of prompt (Φ_{PF}) and delayed (Φ_{DF}) components:

$$\Phi_{\mathrm{TADF}} = \Phi_{\mathrm{PF}} + \Phi_{\mathrm{DF}}$$
$$= \Phi_{\mathrm{PF}} + \Phi_{\mathrm{ISC}}\Phi_{\mathrm{rISC}}\Phi_{\mathrm{PF}} + (\Phi_{\mathrm{ISC}}\Phi_{\mathrm{rISC}})^2\ \Phi_{\mathrm{PF}} + (\Phi_{\mathrm{ISC}}\Phi_{\mathrm{rISC}})^3\ \Phi_{\mathrm{PF}} + \cdots$$

where Φ_{DF} is expanded as an infinite series with terms corresponding to different numbers of rISC/ISC cycles, each terminating in an emission event with the same efficiency as the PF emission.

Summing this infinite geometric series generates:

$$\Phi_{\mathrm{TADF}} = \Phi_{\mathrm{PF}} \frac{1}{1 - \Phi_{\mathrm{ISC}}\Phi_{\mathrm{rISC}}}$$

In a hyperfluorescence system we assume that all photoexcitation is initially on the TADF molecule. At low FE loadings (~1%) this is reasonable, Figure S1. At higher loadings we envision that PLQEs measurements taken relative to samples with equivalent FE loading and thickness but no TADF material (as compared to standard measurements using a blank substrate as reference) should give experimentally access to this modified PLQE value.

In the hyperfluorescence film both emission from the TADF and from the FE following FRET are possible. An expression for the total PLQE (Φ_{HF}) follows:

$$\Phi_{\mathrm{HF}} = \Phi_{\mathrm{PF}} + \Phi_{\mathrm{ISC}}\Phi_{\mathrm{rISC}}\Phi_{\mathrm{PF}} + (\Phi_{\mathrm{ISC}}\Phi_{\mathrm{rISC}})^2\ \Phi_{\mathrm{PF}} + (\Phi_{\mathrm{ISC}}\Phi_{\mathrm{rISC}})^3\ \Phi_{\mathrm{PF}} + \cdots$$
$$+\Phi_{\mathrm{FRET}}\Phi_{\mathrm{FE}} + \Phi_{\mathrm{ISC}}\Phi_{\mathrm{rISC}}\Phi_{\mathrm{FRET}}\Phi_{\mathrm{FE}} + (\Phi_{\mathrm{ISC}}\Phi_{\mathrm{rISC}})^2\Phi_{\mathrm{FRET}}\Phi_{\mathrm{FE}} + \cdots$$

where the two infinite series represent emission by the TADF following some number of rISC/ISC cycles, or emission from the FE material (with quantum efficiency Φ_{FE}) following some number of rISC/ISC cycles terminated by FRET (with efficiency Φ_{FRET}).

As with the TADF material alone, these infinite geometric series can be summed:

$$\Phi_{\mathrm{HF}} = (\Phi_{\mathrm{PF}} + \Phi_{\mathrm{FRET}}\Phi_{\mathrm{FE}})\frac{1}{1 - \Phi_{\mathrm{ISC}}\Phi_{\mathrm{rISC}}}$$

We then express Φ_{PF}, Φ_{FRET}, Φ_{ISC}, and Φ_{rISC} as ratios of rates for processes that can act on the relevant electronic states. For the singlet state the relevant rates are those of fluorescence (yielding Φ_{PF}), ISC, FRET, and nonradiative decay. For the triplet state these are rISC and DET. We approximate the rates of FRET and DET as first order in FE concentration, and neglect other non-radiative processes from the triplet excited state (justified by time-resolved photoluminescence fitting and transient absorption experiments of the TADF material previously reported in 10.1021/acs.jpcc.8b11020). Expanding the previous expression generates:

$$\Phi_{\mathrm{HF}} = \frac{k_F + \Phi_{\mathrm{FE}} k_{FRET}[FE]}{k_F + k_{ISC} + k_{FRET}[FE] + k_{NR}} \left(\frac{1}{1 - \left(\frac{k_{ISC}}{k_F + k_{ISC} + k_{FRET}[FE] + k_{NR}}\right) \times \left(\frac{k_{rISC}}{k_{rISC} + k_{dex}[FE]}\right)} \right)$$

And simplifying:

$$\Phi_{\mathrm{HF}} = \frac{k_F + \Phi_{\mathrm{FE}} k_{FRET}[FE]}{k_F + k_{ISC} + k_{FRET}[FE] + k_{NR} - \frac{k_{ISC}k_{rISC}}{k_{rISC} + k_{dex}[FE]}}$$

where k_F is the rate of fluorescence for the TADF material, k_{FRET} is the rate coefficient of FRET, $[FE]$ is the concentration of the FE, k_{ISC} is the rate of ISC, k_{NR} is the rate of nonradiative transitions from the TADF singlet state, k_{rISC} is the rate of rISC, and k_{dex} is the rate coefficient of DET.

The above expression allows us to model the expected hyperfluorescence film PLQE in terms of the rates of FRET and DET, alongside other rates intrinsic to the TADF material (many of which have already been established for our studied TADF material, 10.1021/acs.jpcc.8b11020).

In several limiting cases this expression is found to conform to expectations. For example, if k_{FRET} is large enough to dominate the denominator, FRET becomes 100% efficient and the entire expression collapses to $\Phi_{\mathrm{HF}} = \Phi_{\mathrm{FE}}$, with all emission occurring from the FE molecules. Alternatively, if k_{dex} dominates all triplets get quenched, and the expression simplifies to $\Phi_{\mathrm{HF}} = \Phi_{\mathrm{PF}} + \Phi_{\mathrm{FRET}}\Phi_{\mathrm{FE}}$.

Comparing Model to Data –To evaluate how this expression behaves and compare it to the experimental PLQE data in Figure 4, we first set several of the rate constants and coefficients that are available from independent means. From previous investigations of this specific TADF emitter at the same concentration in DPEPO host we can set $k_F = 1.5 \times 10^7$, $k_{ISC} = 3.2 \times 10^7$, and $k_{rISC} = 9.8 \times 10^5$ (10.1021/acs.jpcc.8b11020). Furthermore, we are able to determine $k_{NR} = 2.7 \times 10^6$ by varying this parameter until the model $\Phi_{\mathrm{HF}}|_{[FE]=0} = \Phi_{\mathrm{TADF}}$ matches the experimental value of 0.85 (Figure 4a). Φ_{FE} is measured independently, Figure 4a. We are also able to estimate $k_{FRET} = 2.78 \times 10^5\ \%^{-1}$ by considering the changes in decay rate of the PF emission (Figure 3c) across the range of [FE] concentrations studied. An interactive spreadsheet is included as additional SI material that allows the effects on model PLQE to be determined as various parameters are changed.

In the main text we propose that two distinct FRET rates exist - a faster one for the PF representing the bulk-average of TADF-FE distances, and a slower one in the DF corresponding a subset of TADF molecules more distance from any FE (which allow them to undergo ISC). It is unclear how to incorporate this time-dependant FRET rate into the steady-state model equation in a simple way. Potentially this could be included as a geometrically decreasing prefactor in the $(\Phi_{\mathrm{ISC}}\Phi_{\mathrm{rISC}})^{\mathrm{n}}\Phi_{\mathrm{FRET}}\Phi_{\mathrm{FE}}$ terms in the above infinite sum for Φ_{HF}, indicating that Φ_{FRET} gets less efficient on subsequent (later) cycles as slower FRET acts on more isolated TADF molecules. Nonetheless we note that the coincidental feature of our chosen material system that $\Phi_{\mathrm{TADF}} = \Phi_{\mathrm{FE}}$ makes this modification unnecessary here. Because both materials emit with the same efficiency, the ratio of TADF/FE emission in the DF (which would be impacted by the slower FRET rate in the DF), has no influence on the recorded total PLQE in this case.

Together the considerations above leave only k_{dex} as a free parameter. Fitting to minimise residuals between the model and the data in Figure 4 immediately finds a best-fit value of $k_{dex} = 0$. Similar fitted values are also converged on when k_{FRET} – the only other parameter not intrinsic to the TADF material – is allowed to vary. This corresponds to a situation where only FRET is active, which is fully consistant with the absence of a dip in PLQE values at intermediate [FE] concentrations in experiments. The expected behaviour if DET were active is a drop in PLQE as it competes with rISC, but then for Φ_{HF} to approach Φ_{FE} as [FE] increases, as FRET begins to outcompete k_F and k_{ISC}.

Furthermore, if we consider the changes in DF rate (which for equivalent changes in [FE] are ~145 times slower than those in the PF which we attribute to FRET, Figure 3c) and deliberately misattribute these changes in DF rate to DET, they yield a value of $k_{dex} = 1.9 \times 10^5\ \%^{-1}$. However setting this value for k_{dex} gives very poor agreement with the data (Figure 4b, blue curve), indicating that this DF quenching cannot be attributed to DET.

Acknowledging that the error bars in Figure 4 are substantial, we can also estimate an upper bound for k_{dex} that still agrees with our data within those bounds. However doing so results in a rather low value of $k_{dex} = 6 \times 10^4\ \%^{-1}$, corresponding to DET rates no greater than 3×10^5 even for the sample with [FE] = 5%, which would be expected to have the fastest DET. This rate of DET though is outcompeted by rISC on the TADF molecule itself, and so even in this best-case scenario for DET (while remaining consistent with the PLQE results), this process cannot be responsible for the changes in DF rate that we observe. Instead we propose a distribution of FRET rates, as discussed in the main text.